Converting Baluns Into Broad-Band Impedance-Transforming 180° Hybrids

Kian Sen Ang, *Member, IEEE,* and Yoke Choy Leong

***Abstract*—A technique for converting baluns into 180° hybrids by adding an in-phase power splitter is presented in this paper. Incorporating the broad-band antiphase and in-phase power splitting characteristics of the balun and power splitter results in a 180° hybrid with broad-band characteristics. This technique also provides a means of achieving perfect matching and output isolation for three-port lossless baluns. Applying this technique to a Marchand balun will result in a broad-band impedance-transforming 180° hybrid. Simple design equations based on the scattering matrix are presented. These theoretical results are validated by an experimental 180° hybrid using a coupled line Marchand balun. It achieves amplitude balance of 0.5 dB and phase balance of less than 5° from 1.2 to 3.2 GHz.**

***Index Terms*—Baluns, impedance transformation, Marchand baluns, 180° hybrids.**

I. Introduction

THE 180° hybrid ring is a fundamental component in microwave circuits. It performs the important function of in- and out-of-phase power splitting while maintaining perfectly matched ports. Compared to the 90° branch-line coupler, it has broader bandwidth [1] and the isolation between the input ports may be independent of the output termination impedances. Therefore, the 180° hybrid ring is extensively used for isolated power splitting in balanced mixers, multipliers, power amplifiers, and antenna feed networks.

The conventional 180° hybrid ring, as shown in Fig. 1(a), is inherently a narrow-band structure. Previous papers [2]–[6] has attributed this bandwidth limitation to the narrow-band $\lambda/2$ phase inverter within the $3\lambda/4$ line section. Consequently, March [2] replaced the $3\lambda/4$ section with a $\lambda/4$ coupled line section, which has broad-band phase inversion characteristics, as shown in Fig. 1(b). Although the bandwidth increases considerably, the even-mode impedance required for the coupled section is too extreme to be realized on commonly used microstrip circuits. Others [3]–[5] replaced the $\lambda/2$ line in the $3\lambda/4$ section with broad-band phase inverters, which cannot be implemented on microstrip circuits. In addition to using broad-band phase inverters, quarter-wavelength impedance transformers have also been added to the hybrid ring for bandwidth improvement [6], but this increases the overall circuit size and requires a very low-impedance line section.

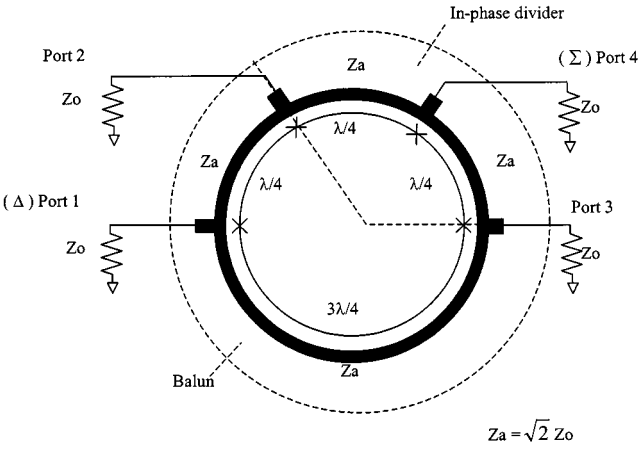

(a)

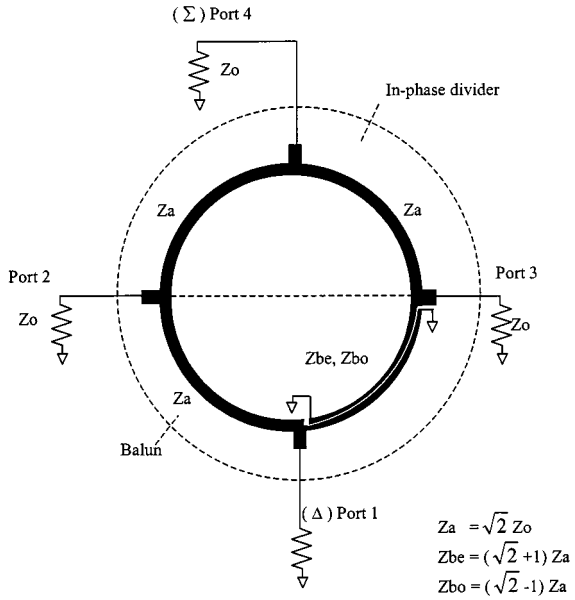

(b)

Fig. 1. (a) Conventional hybrid ring. (b) Modified hybrid ring proposed by March [2].

In this paper, new insight into the bandwidth limitation of the hybrid ring is presented. It will be shown that the bandwidth of the hybrid ring is limited by the narrow-band nature of the balun operation within the hybrid structure. This leads to the incorporation of broad-band baluns to realize broad-band 180° hybrid structures. It also provides a technique for achieving perfect matching and output isolation in three-port lossless baluns.

Manuscript received September 3, 2001.

The authors are with the Defence Science Organization National Laboratories, Singapore 118230 (e-mail: akiansen@dso.org.sg).

Publisher Item Identifier 10.1109/TMTT.2002.801353.

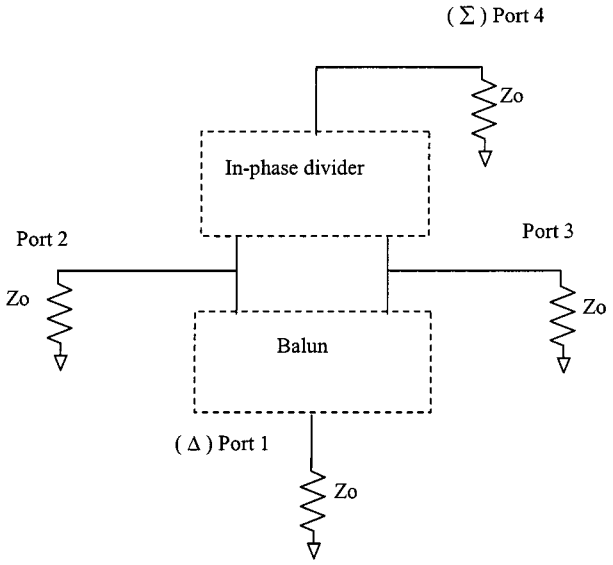

Fig. 2. Conceptual block diagram of a general 180° hybrid.

The design and performance of these balun-incorporated 180° hybrids will be presented in this paper.

II. Concept

The conventional and modified hybrid rings can be partitioned into an in-phase power divider and a balun, as illustrated in Fig. 1. In the conventional hybrid ring of Fig. 1(a), the in-phase power divider consists of a pair of $\lambda/4$ line sections, while the balun consists of a $\lambda/4$ noninverting arm and an inverting $3\lambda/4$ line section. Therefore, although the power divider is a broad-band structure, the bandwidth of the overall hybrid is limited by the narrow-band balun. In the modified hybrid ring of Fig. 1(b), this narrow-band balun is replaced by a broad-band balun consisting of a $\lambda/4$ noninverting arm and a $\lambda/4$ inverting coupled line section.

Therefore, the 180° hybrid can be considered conceptually as a combination of an in-phase power divider and a balun, as depicted in Fig. 2. The power divider provides in-phase power splitting/combining between (sum) port 4 and ports 2 and 3, while the balun provides antiphase power splitting/combining between (delta) port 1 and ports 2 and 3. The basic design requirement is to determine the network properties of the in-phase power divider and balun such that all the ports are matched and opposite ports are isolated for hybrid operation. This can be derived from the two-port even- and odd-mode analysis where the sum and delta ports are terminated. This is illustrated in Fig. 3. Also shown in Fig. 3 are the following even-mode reflection, odd-mode reflection, and transmission coefficients Γe, Γo, Te, and To for ports 2 and 3 in the in-phase power divider and balun

$$\begin{array}{lll} & \underline{\text{In-phase divider}} & \underline{\text{balun}} \\ \text{Even-mode:} & \Gamma e = 0,\, Te = 0 & \Gamma e = 1,\, Te = 0 \\ \text{Odd-mode:} & \Gamma o = 1,\, To = 0 & \Gamma o = 0, To = 0. \end{array} \quad (1)$$

These values are characteristics of the in-phase power divider and the baluns in Fig. 1. Under even-mode excitations in Fig. 3(a), the connections to the balun will appear as open

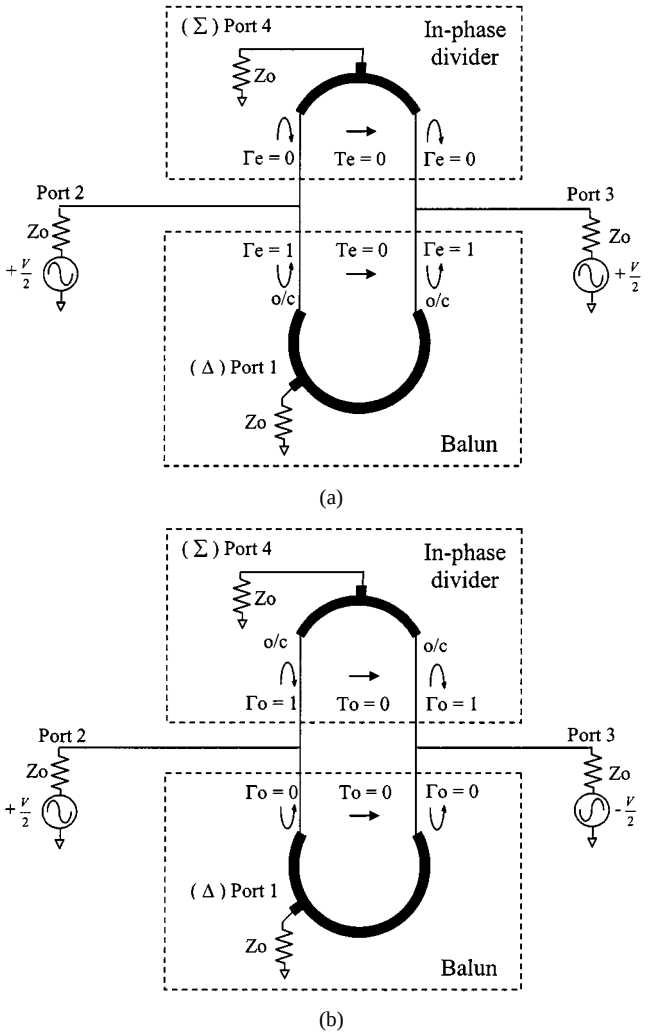

Fig. 3. (a) Even- and (b) odd-mode networks for the general 180° hybrid in Fig. 2.

circuits. Thus, the overall circuit will perform as an in-phase divider with $\Gamma e = 0$ and $Te = 0$. On the other hand, under odd-mode excitations in Fig. 3(b), the in-phase divider terminals will appear as open circuits and only the balun will be in operation with $\Gamma o = 0$ and $To = 0$. Therefore, the resulting circuit functions as an ideal in-phase power divider or balun, depending on the mode of excitation. Summing the results for both excitations also show that ports 2 and 3 are perfectly matched and isolated.

In summary, the requirements for the power divider and balun in the hybrid structure of Fig. 2 are for them to satisfy (1). Note that not every power divider and balun has these properties. For example, the multisection branch-line balun [7], consisting of $\lambda/2$ line sections, which are $\lambda/4$ apart, presents short-circuited terminals under even-mode excitations, instead of open circuits. Similarly, in a two-section lossless $\lambda/4$ power divider, the in-phase terminals present short-circuited terminals under odd-mode excitations. However, these short-circuited terminals can be easily transformed to open circuits by adding $\lambda/4$ transformers to the respective outputs.

Equipped with this new insight, we can replace the baluns in Fig. 1(a) and (b) with other broad-band more realizable baluns

to improve the bandwidth of the hybrid ring. Consequently, this also suggests that, by adding a broad-band in-phase power divider between the output ports of a balun, all the balun ports can be matched and the outputs are isolated, as in the 180° hybrid. In this paper, the impedance-transforming Marchand balun [8] will be employed to implement broad-band 180° hybrids. Therefore, the resulting 180° hybrid will have the additional capability of performing impedance transformation between the input and output ports. This is useful in several applications. For example, an impedance-transforming 180° hybrid can be employed in a balanced mixer to match the local oscillator (LO) and RF port impedances to that of the mixing diodes. In a push–pull amplifier, the use of a balun with matched and isolated outputs can enhance amplifier stability.

III. Analysis

When (1) is satisfied, the three-port balun and in-phase power divider, with port definitions given in Fig. 2, can be characterized by their S matrices

$$S_{\text{balun}} = \begin{bmatrix} 0 & S_{12} & -S_{12} \\ S_{12} & \frac{1}{2} & \frac{1}{2} \\ -S_{12} & \frac{1}{2} & \frac{1}{2} \end{bmatrix} \quad S_{\text{divider}} = \begin{bmatrix} 0 & S_{12} & S_{12} \\ S_{12} & \frac{1}{2} & -\frac{1}{2} \\ S_{12} & -\frac{1}{2} & \frac{1}{2} \end{bmatrix}. \tag{2}$$

In addition, S_{balun} and S_{divider} are both unitary matrices to satisfy the lossless condition, giving

$$|S_{12}| = \frac{1}{\sqrt{2}}. \tag{3}$$

These are the optimum S matrices for the three-port networks. They are matched at the input and have transmission coefficients of -3 dB, which are opposite phase for the balun and in-phase for the power divider. The outputs, however, are not matched or isolated. Both the output matching and isolation have a value of -6 dB.

When these two networks are connected back-to-back, as in Fig. 2, the S matrix of the resulting four-port network can be derived using the multiport connection method [9]. The result is as follows:

$$S_{\text{hybrid}} = \begin{bmatrix} \overbrace{\begin{matrix} 0 & S_{12} & -S_{12} & 0 \\ S_{12} & 0 & 0 & S_{12} \\ -S_{12} & 0 & 0 & S_{12} \\ 0 & S_{12} & S_{12} & 0 \end{matrix}}^{S'_{\text{balun}}} \\ \underbrace{\qquad\qquad\qquad\qquad}_{S'_{\text{divider}}} \end{bmatrix}. \tag{4}$$

The resulting S matrix composes of S'_{balun} and S'_{divider}, which are, respectively, the S matrices of an ideal balun and power divider. Therefore, by combining the balun and in-phase power divider, their individual antiphase and in-phase power splitting characteristics with matched inputs are maintained. In addition, their output ports are now perfectly matched and isolated. Moreover, the balun input is also isolated from the power-divider input. In fact, S_{hybrid} can be identified as the S matrix of an ideal 180° hybrid.

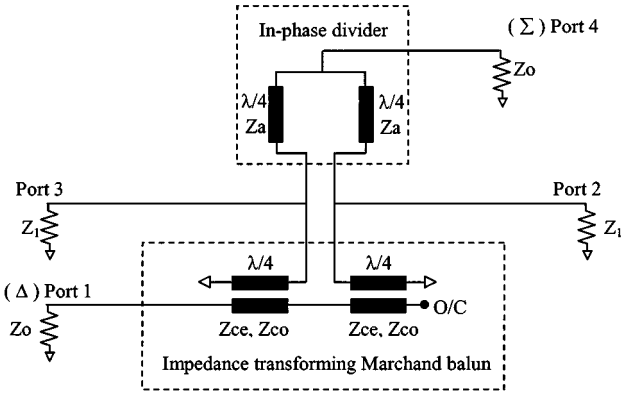

Fig. 4. Block diagram of an impedance-transforming 180° hybrid employing a Marchand balun.

Therefore, the basic design requirement of the balun and in-phase power divider is for them to have the optimum S matrices given in (2). For the power dividers in Fig. 1, which consists of a pair of $\lambda/4$ line sections of impedance Z_a, the S matrix is given by

$$S_{\text{divider}} = \begin{bmatrix} \frac{z_a^2 - 2z_0^2}{z_a^2 + 2z_0^2} & -j\frac{2z_a z_0}{z_a^2 + 2z_0^2} & -j\frac{2z_a z_0}{z_a^2 + 2z_0^2} \\ -j\frac{2z_a z_0}{z_a^2 + 2z_0^2} & \frac{z_a^2}{z_a^2 + 2z_0^2} & \frac{-2z_0^2}{z_a^2 + 2z_0^2} \\ -j\frac{2z_a z_0}{z_a^2 + 2z_0^2} & \frac{-2z_0^2}{z_a^2 + 2z_0^2} & \frac{z_a^2}{z_a^2 + 2z_0^2} \end{bmatrix}. \tag{5}$$

To obtain the desired S_{divider} given in (2), the required line impedance is given by $Z_a = \sqrt{2}Z_0$. This impedance value is consistent with that of the power dividers given in Fig. 1.

Fig. 4 shows the block diagram of an impedance-transforming 180° hybrid employing a coupled line Marchand balun. In this hybrid structure, the source impedances Z_0 at ports 1 and 4 can be transformed to match the load impedances Z_1 at ports 2 and 3.

With these port impedances, the S matrix of the in-phase power divider becomes

$$S_{\text{divider}} = \begin{bmatrix} \frac{z_a^2 - 2z_0 z_1}{z_a^2 + 2z_0 z_1} & -j\frac{2z_a\sqrt{z_0 z_1}}{z_a^2 + 2z_0 z_1} & -j\frac{2z_a\sqrt{z_0 z_1}}{z_a^2 + 2z_0 z_1} \\ -j\frac{2z_a\sqrt{z_0 z_1}}{z_a^2 + 2z_0 z_1} & \frac{z_a^2}{z_a^2 + 2z_0 z_1} & \frac{-2z_0 z_1}{z_a^2 + 2z_0 z_1} \\ -j\frac{2z_a\sqrt{z_0 z_1}}{z_a^2 + 2z_0 z_1} & \frac{-2z_0 z_1}{z_a^2 + 2z_0 z_1} & \frac{z_a^2}{z_a^2 + 2z_0 z_1} \end{bmatrix}. \tag{6}$$

In this case, the required line impedance to achieve the S_{divider} matrix in (2) is given by

$$Z_a = \sqrt{2Z_0 Z_1}. \tag{7}$$

Similarly, the baluns in Fig. 1(a) and (b) can also be designed for impedance transformation from Z_0 to Z_1 by satisfying (7). In this

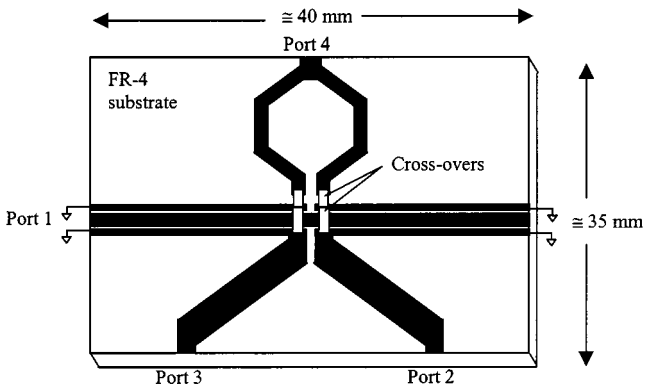

Fig. 5. Layout of the fabricated broad-band balun/180° hybrid.

paper, however, the impedance-transforming Marchand balun [8] will be employed. It consists of two $\lambda/4$ coupled line sections, in which the unconnected ports are terminated in short and open circuits, as shown in Fig. 4. The required even- and odd-mode impedances for the coupled line sections are given by

$$Z_{ce} = Z_0\sqrt{\frac{1+C}{1-C}} \quad Z_{co} = Z_0\sqrt{\frac{1-C}{1+C}} \tag{8}$$

where C is the coupling factor of the coupled lines.

For the balun to transform from source impedance of Z_0 to load impedances Z_1, the required coupling factor is given by [8]

$$C = \sqrt{\frac{Z_0}{Z_0 + 2Z_1}}. \tag{9}$$

When (8) and (9) are satisfied, the S_{balun} matrix required in (2) for the Marchand balun will be obtained.

Equations (7)–(9) present the required design equations for the impedance-transforming 180° hybrid based on the coupled-line Marchand baluns. For the case where $Z_0 = Z_1 = 50\,\Omega$, the required coupling factor is -4.8 dB and the even- and odd- mode impedances are $Z_{ce} = 97\,\Omega$ and $Z_{co} = 26\,\Omega$. Compared to the impedances of $Z_{be} = 170.7\,\Omega$ and $Z_{bo} = 29.3\,\Omega$, required by the modified hybrid ring in Fig. 1(b), these values are more realizable in microstrip coupled lines.

Although the analysis is only performed at the center frequency of operation, the results are valid over a relatively broad bandwidth due to the broad-band nature of the in-phase power divider and balun.

IV. Experimental Results

To validate the analytical results and demonstrate the proposed technique, a broad-band microstrip 180° hybrid based on the Marchand coupled-line balun was designed. The circuit layout is shown in Fig. 5. The circuit was fabricated on a low-cost FR-4 board with a dielectric constant of 4.4 and a thickness of 1.6 mm. The coupled line sections were realized using three-conductor coupled lines [10]. The conductor widths for the center conductor and the two side conductors are, respectively, 1 and 0.5 mm, while the gaps between them are 0.1 mm. The conductor width for the two power divider arms is

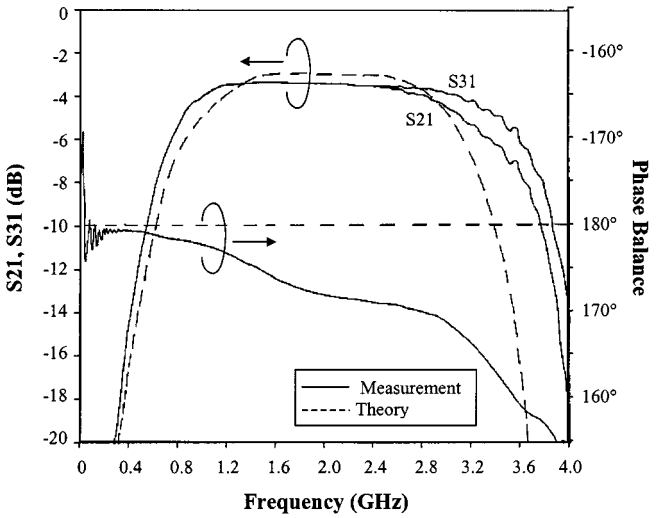

Fig. 6. Measured and theoretical coupling parameters of the Marchand balun without a power-divider network.

1 mm. Quarter-wavelength for the designed frequency of 2 GHz is approximately 20 mm. Sections of 50-Ω microstrip lines were used to extend ports 2 and 3 for measurement. The microstrip traces were defined by a T-tech printed-circuit board (PCB) router. The crossovers were implemented by soldering stripes of copper tape across the microstrip traces. The short circuits for the coupled lines were obtained by soldering strips of copper around the edge of the substrate. The overall circuit size is approximately 40×35 mm^2.

The layout of Fig. 5 illustrates that the input–output ports of the resulting 180° hybrid are no longer constrained to be alternating around a ring, as in the conventional hybrid ring. This presents a more convenient and versatile layout for many applications. For example, when employed in a balanced diode mixer, the LO and RF can be conveniently applied to the adjacent ports 1 and 4, while the diode pair can be directly mounted at the balun outputs.

The fabricated circuit was first measured as a balun, without the crossovers to the in-phase power divider, to verify the performance of the Marchand balun. Fig. 6 shows the measured and theoretical balun coupling parameters. The theoretical responses are based on simulations using Agilent's ADS software,[1] with ideal transmission lines and ideal coupled line sections defined by (7)–(9). The measured passband is wider than the theoretical one, probably due to the slight over-coupling in the three-line microstrip couplers. The measured passband is flat from 1 to approximately 3 GHz with approximately -0.5-dB insertion loss. Both $|S21|$ and $|S31|$ track each other as in the theoretical curves, except at the high-frequency end of the passband. This increasing amplitude imbalance at high frequencies can be attributed to the unequal even- and odd-mode phase velocities in the nonhomogeneous microstrip coupled lines. Similarly, although theoretical phase balance is perfect for all frequencies, measured phase imbalance increases with frequency, to approximately 10° at the upper end of the passband. Fig. 7 shows the return loss and output isolation of the balun. The input is well matched within the balun passband. The output return losses and

[1]Agilent Technol. Advanced Design Syst. v1.3, Palo Alto, CA, 1999.

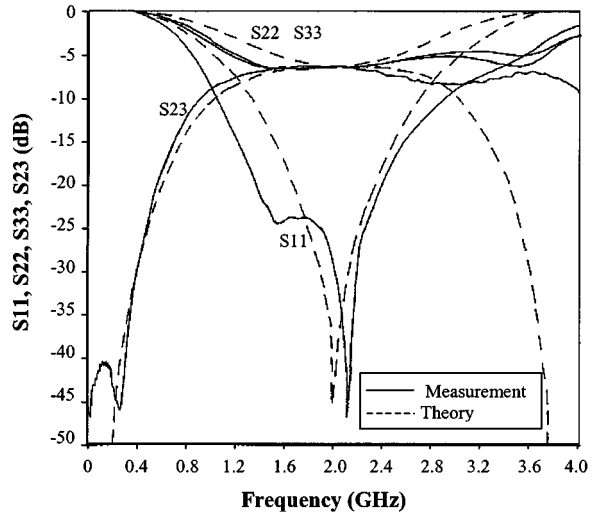

Fig. 7. Measured and theoretical return loss and output isolation of Marchand balun without a power-divider network.

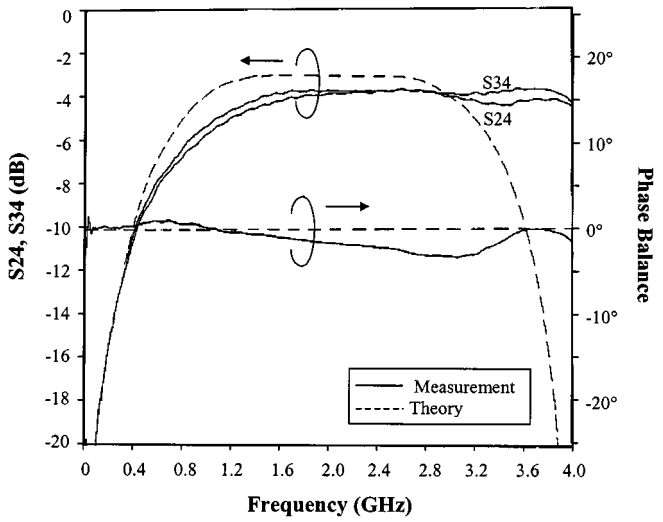

Fig. 9. Measured and theoretical coupling parameters for the sum port of the 180° hybrid.

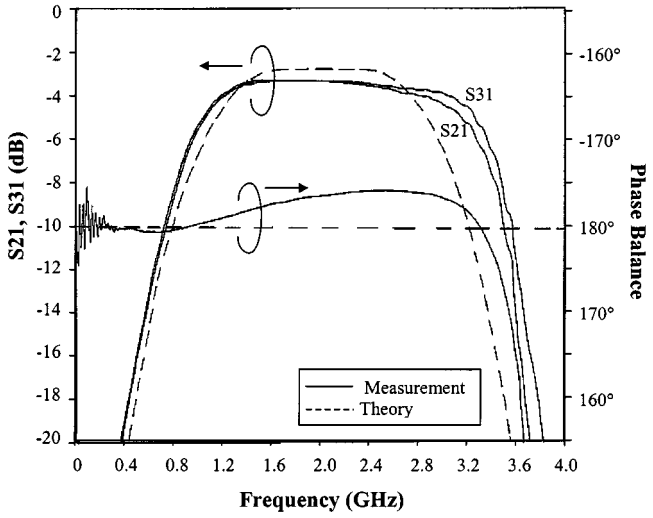

Fig. 8. Measured and theoretical coupling parameters for the delta port of the 180° hybrid.

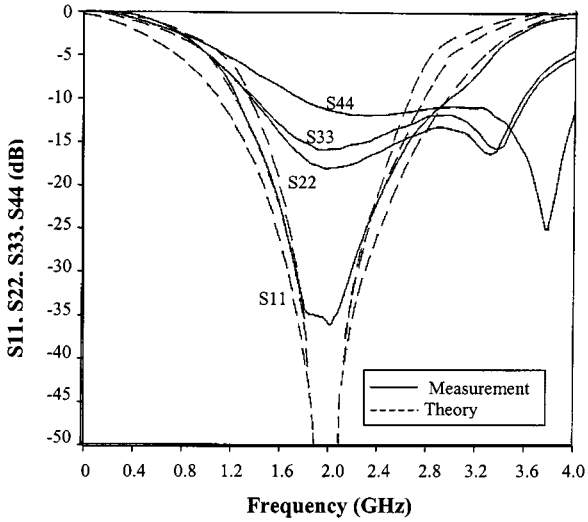

Fig. 10. Measured and theoretical return loss for all the ports of the 180° hybrid.

isolation hovers around −6 dB, which is in agreement with the theoretical curves.

Having verified the balun performance, the crossovers between the balun and power divider are then added to measure the performance of the resulting 180° hybrid. Fig. 8 shows the coupling parameters for the delta port of the hybrid. Comparing Figs. 6 and 8, there is a slight decrease in the measured bandwidth at the edges of the passband, just as in the theoretical bandwidth. The measured phase balance, however, has improved to less than 5° within the passband. Fig. 9 shows the corresponding coupling parameters for the sum port. Similarly, the two coupling parameters $S24$ and $S34$ track each other closely and the phase balance is less than 5° throughout the measurement frequency range. It is also evident that the bandwidth of the in-phase power divider is much wider than that of the balun. Therefore, the overall bandwidth of the 180° hybrid can be further increased by improving the bandwidth of the balun employed.

Fig. 10 shows the return loss of all the ports of the 180° hybrid. Comparing Figs. 10 and 7, the delta input remains well matched within the passband, as in the balun without the power-divider network. The measured return loss $S22$ and $S33$ has improved from −6 dB in Fig. 7 to better than −12 dB within the passband. The measured return loss for the sum port is better than −10 dB. The improvement in these measured return losses are less than theoretical, which is likely due to the parasitic effects of the crossovers in the power-divider circuit.

The port isolations are shown in Fig. 11. The measured isolation between ports 2 and 3 has improved from −6 dB in Fig. 6 to better than −15 dB within the passband. The sum and delta port isolation is theoretically infinite due to the perfect amplitude and phase balances. This can only be achieved at low frequencies and the measured isolation degrades to approximately −30 dB at the high-frequency end of the passband.

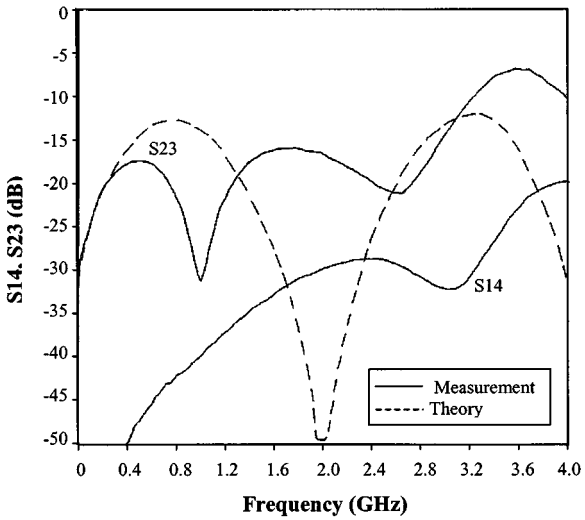

Fig. 11. Measured and theoretical port isolations of the 180° hybrid.

V. Conclusion

The conventional hybrid ring has been identified as a combination of an in-phase power divider and a balun. This resulted in a technique for converting baluns into broad-band 180° hybrids. It also provides a means of achieving output matching and isolation for lossless three-port baluns. This technique has been applied to the impedance-transforming Marchand balun for the implementation of impedance-transforming 180° hybrids. Simple design equations based on an S matrix have been derived. Based on these results, a broad-band 180° hybrid has been realized using Marchand coupled-line baluns. Capitalizing on the broad-band characteristics of the balun, the fabricated 180° hybrid exhibits a wide bandwidth of almost 100% with amplitude and phase balance of less that 0.5 dB and 5°, respectively. Measured results also show that the bandwidth of the proposed 180° hybrid can be further increased by employing baluns of even wider bandwidth.

Acknowledgment

The authors would like to thank K. K. Ang, DSO National Laboratories, Singapore, for his technical support in the circuit fabrication.

References

[1] C. Y. Pon, "Hybrid-ring directional coupler for arbitrary power divisions," *IRE Trans. Microwave Theory Tech.*, vol. MTT-9, pp. 529–535, Nov. 1961.

[2] S. March, "A wideband stripline hybrid ring," *IEEE Trans. Microwave Theory Tech.*, vol. MTT-16, p. 361, June 1968.

[3] S. Rehnmark, "Wide-band balanced line microwave hybrids," *IEEE Trans. Microwave Theory Tech.*, vol. MTT-25, pp. 825–830, Oct. 1977.

[4] T. Wang and K. Wu, "Size-reduction and band-broadening design technique of uniplanar hybrid ring coupler using phase inverter for M(H)MIC's," *IEEE Trans. Microwave Theory Tech.*, vol. 47, pp. 198–206, Feb. 1999.

[5] C. Y. Chang and C. C. Yang, "A novel broad-band Chebyshev-response rat-race ring coupler," *IEEE Trans. Microwave Theory Tech.*, vol. 47, pp. 455–462, Apr. 1999.

[6] D. I. Kim and Y. Naito, "Broad-band design of improved hybrid ring 3-dB directional couplers," *IEEE Trans. Microwave Theory Tech.*, vol. MTT-30, pp. 2040–2046, Nov. 1982.

[7] R. Knochel, B. Mayer, and U. Goebel, "Unilateral microstrip balanced and doubly balanced mixers," in *IEEE Int. Microwave Symp. Dig.*, 1989, pp. 1247–1250.

[8] K. S. Ang and I. D. Robertson, "Analysis and design of impedance-transforming planar Marchand baluns," *IEEE Trans. Microwave Theory Tech.*, vol. 49, pp. 402–406, Feb. 2001.

[9] J. A. Dobrowolski, *Introduction to Computer Methods for Microwave Circuit Analysis and Design*. Norwood, MA: Artech House, 1991, pp. 81–90.

[10] S. A. Maas and K. W. Chang, "A broadband, planar, doubly balanced monolithic Ka-band diode mixer," *IEEE Trans. Microwave Theory Tech.*, vol. 41, pp. 2330–2335, Dec. 1993.

Kian Sen Ang (M'02) was born in Singapore, in 1969. He received the B.Eng. degree from the National University of Singapore, Singapore, in 1994, and Ph.D. degree from the University of Surrey, Surrey, U.K. in 2000.

In 1994, he joined the Defence Science Organization (DSO), Singapore, as a Research Engineer involved in microwave circuit and sub-system designs. He is currently a Senior Member of Technical Staff with the DSO National Laboratories. His research interests include design, analysis, and measurement of novel microwave circuits including monolithic integrated circuits. He has authored over 20 publications in this area and was a contributing author of *RFIC and MMIC Design and Technology* (London, U.K.: IEE Press, 2001).

Yoke Choy Leong received the B.Eng. (with honors) and M.Sc. degrees from the National University of Singapore, Singapore, in 1991 and 1995, respectively, and the Ph.D. degree from the University of Massachusetts Amherst, in 2000.

Since 1991, he has been with the Defence Science Organization (DSO) National Laboratories, Singapore, where he is involved in the area of microwave component and system design. His research interest is in microwave/millimeter-wave monolithic microwave integrated circuit (MMIC) design and modeling, analysis, and synthesis of novel passive structures.